17

Fuzzy Control Strategy for Cooperative Non-holonomic Motion of Cybercars with Passengers Vibration Analysis

Francesco Maria Raimondi and Maurizio Melluso
Dipartimento di Ingegneria dell'Automazione e dei Sistemi, University of Palermo
Italy

1. Introduction

The cybercars are electric road wheeled non-holonomic vehicles with fully automated driving capabilities. They contribute to sustainable mobility and are employed as passenger vehicles. Non-holonomic mechanics describes the motion of the cybercar constrained by non-integrable constraints, i.e. constraints on the system velocities that do not arise from constraints on the configuration alone. First of all there are thus with dynamic non-holonomic constraints, i.e. constraints preserved by the basic Euler-Lagrange equations (Bloch, 2000; Melluso, 2007; Raimondi & Melluso, 2006-a). Of course, these constraints are not externally imposed on the system but rather are consequences of the equations of motion of the cybercar, and so it sometimes convenient to treat them as conservation laws rather than constraints per se. On the other hand, kinematic non-holonomic constraints are those imposed by kinematics, such as rolling constraints. The goal of the motion control of cybercars is to allow the automated vehicle to go from one terminal to another while staying on a defined trajectory and maintaining a set of performance criteria in terms of speeds, accelerations and jerks. There are many results concerning the issue of kinematic motion control for single car (Fierro & Lewis, 1997). The main idea behind the kinematic control algorithms is to define the velocity control inputs which stabilize the closed loop system. These works are based only on the steering kinematics and assume that there exists perfect velocity tracking, i.e. the control signal instantaneously affects the car velocities and this is not true. Other control researchers have target the problems of time varying trajectories tracking, regulating a single car to a desired position/orientation and incorporating the effects of the dynamical model to enhance the overall performance of the closed loop system. The works above are based on a backstepping approach, where the merging of kinematic and dynamic effects leads to the control torques applied to the motors of the wheels. A Fuzzy dynamic closed loop motion control for a single non-holonomic car based on backstepping approach and oriented to stability analysis of the motion errors has been developed by Raimondi & Melluso (2005). In Raimondi & Melluso (2006-b) and Raimondi & Melluso (2007-a) adaptive fuzzy motion control systems for single non-holonomic automated vehicles with unknown dynamic and kinematic parameters and Kalman's filter to localize the car have been presented. With regards to the problems of cooperative control of multiple cybercars, a number of techniques have been developed for omni-directional

Source: Motion Control, Book edited by: Federico Casolo,
ISBN 978-953-7619-55-8, pp. 580, January 2010, INTECH, Croatia, downloaded from SCIYO.COM

(holonomic) wheeled cars (see Gerkey & Mataric, 2002; La Valle & Hutchinson, 1998). Decentralized algorithms have been dealt with for holonomic cars by Lumelsky & Harinarayan (1997). With regards to the cooperation of multiple non-holonomic cybercars, few results have been published. On this subject, an approach based on the definition of suitable functions of inverse kinematics to control the motion of a platoon of autonomous vehicles has been presented by Antonelli & Chiaverini (2006). The problem of controlling multiple non-holonomic vehicles by using fuzzy control so that they converge to a source has been studied by Driessen *et al,* (1999). However, since the cars do not have passengers on board, all the studies above do not consider the problem of the acceleration and jerk. For fully automated operation with passengers, a trajectory planning method that produces smooth trajectories with low acceleration is required. The jerk, i.e. the derivative of the acceleration, adversely affects the efficiency of the control algorithms and passengers comfort, so that it has to be reduced. Not many results have been published on this subject (Labakhua *et al.,* 2006; Panfeng *et al.,* 2007).

In this chapter a new closed loop fuzzy control system for non-holonomic motion of multiple cybercars in presence of passengers is proposed. The control strategy merges an innovative decentralized planning trajectory algorithm and a new fuzzy motion control law. About the cooperation, if the target position is fixed, then a number of cybercars has to reach the target one, without to come into collision with the other closest vehicles. The trajectories are planned as the desired time evolution for the position and orientation of some representative point of each cybercar. Forward trajectories are planned only, i.e. trajectories without manoeuvres. In other words all the cooperative cybercars should not stop, except, of course, at the initial and final position. Therefore circular trajectories with continuous curvature have been chosen. Since, for example, in airport the cybercars move in preferential roads without obstacles, the environment in which they move is considered free of obstacle. To ensure the trajectory tracking of all the cooperative cybercars, a new control strategy based on fuzzy inference system is proposed and developed. The fuzzy system generates the control torques for all the cybercars. The cybercars are still employed to transport passengers which are inevitable exposed to vibrations (Birlik & Sezgin, 2007). The acceleration is adopted as preferred measurement of the human vibration exposure. Therefore, with respect to other control theories, the parameters of the fuzzy controller developed in this chapter may be tuned with respect of the ISO 2631-1 standard, which proposes a comfort scale using a mean acceleration index.

This chapter is organized as follows. Section 2 presents the dynamical model of multiple cybercars which has to be employed to project the dynamic fuzzy control system. Also the acceleration model is formulated to develop a control strategy where the passenger comfort is ensured. Section 3 presents a new decentralized cooperative trajectory planner, where the aim is that all the cybercars must reach a target position without collisions between them. Section 4 presents the closed loop fuzzy motion control system, where the asymptotical stability of the motion errors given by the difference between the reference trajectory planned in Section 3 and the actual trajectory of each cybercar is proved by using the Lyapunov's theorem and the Barbalat's Lemma (Slotine & Li, 1991). The parameters of the fuzzy control law are investigated to ensure a good level comfort of the passengers. In this sense, the adjustment of the saturation values of the fuzzy dynamic control surfaces guarantees low values of the longitudinal, lateral accelerations and jerks. In Section 5 experimental tests in a Matlab environment are employed to confirm the effectiveness of the proposed motion control strategy. Some conclusions are drawn in Section 6.

2. Model formulation of multiple non-holonomic cybercars

Consider a system made up of *r* non-holonomic cybercars. A schematization of the system in open chain configuration is shown in Fig. 1. Now indicating with $\mathbf{q}_i(t) \in R^n$ the time varying coordinates of the position and orientation of the *i*-cybercar,

Fig. 1. System of *r* vehicles in open chain configuration

the complete system is subject to $r \times m$ non-holonomic constraints given by:

$$\boldsymbol{\rho}(\mathbf{q}_1(t), \mathbf{q}_2(t), ..., \mathbf{q}_r(t), \dot{\mathbf{q}}_1(t), \dot{\mathbf{q}}_2(t), ..., \dot{\mathbf{q}}_r(t)) = \mathbf{0}, \tag{1}$$

where:

$$\boldsymbol{\rho}(\mathbf{q}_1(t), \mathbf{q}_2(t), ..., \mathbf{q}_r(t), \dot{\mathbf{q}}_1(t), \dot{\mathbf{q}}_2(t), ..., \dot{\mathbf{q}}_r(t)) = \begin{bmatrix} \mathbf{A}_1(\mathbf{q}_1(t))\dot{\mathbf{q}}_1(t) \\ \mathbf{A}_2(\mathbf{q}_2(t))\dot{\mathbf{q}}_2(t) \\ \cdots \\ \mathbf{A}_\mathbf{r}(\mathbf{q}_r(t))\dot{\mathbf{q}}_r(t) \end{bmatrix} \tag{2}$$

and $\mathbf{A}_i(\mathbf{q}_i(t)) \in R^{m \times n}$ are the matrices of the non-holonomic constraints of the motion of each vehicle. Consider the following well known dynamic model (Fierro & Lewis , 1997) :

$$\mathbf{M}_i(\mathbf{q}_i(t))\ddot{\mathbf{q}}_i(t) + \mathbf{C}_i(\mathbf{q}_i(t), \dot{\mathbf{q}}_i(t))\dot{\mathbf{q}}_i(t) = \mathbf{E}_i(\mathbf{q}_i(t))\boldsymbol{\tau}_i(t) - \mathbf{A}_i^{\mathbf{T}}(\mathbf{q}_i(t))\boldsymbol{\lambda}_i, \tag{3}$$

$$i = 1...r,$$

where $\mathbf{M}_i(\mathbf{q}_i(t)) \in R^{n \times n}$ is a positive definite inertial matrix, $\mathbf{C}_i(\mathbf{q}_i(t), \dot{\mathbf{q}}_i(t)) \in R^{n \times n}$ is the centripetal Coriolis matrix, $\boldsymbol{\tau}_i(t) \in R^p$ is a vector of the torques applied to the right and left wheels of each vehicle, $\mathbf{E}_i(\mathbf{q}_i(t)) \in R^{n \times p}$ is a mapping between the torques above and the forces applied along the components of $\mathbf{q}_i(t)$, $\mathbf{A}_i(\mathbf{q}_i(t))$ are the matrices given by (2), while $\boldsymbol{\lambda}_i \in R^m$ is a vector of Lagrange multipliers. Let $\mathbf{S}_i(\mathbf{q}_i(t)) \in R^{n \times (n-m)}$ be a full rank matrix made up of a set of smooth and linearly independent vectors spanning the null space of $\mathbf{A}_i(\mathbf{q}_i(t))$, i.e.:

$$\mathbf{A}_i(\mathbf{q}_i(t))\mathbf{S}_i(\mathbf{q}_i(t)) = \mathbf{0}, i = 1...r. \tag{4}$$

Due to the non-holonomic constraints (1), it is possible to find velocity vectors $\mathbf{v}_i(t) \in R^{n-m}$, such that:

$$\dot{\mathbf{q}}_i(t) = \mathbf{S}_i(\mathbf{q}_i(t))\mathbf{v}_i(t), i = 1...r. \tag{5}$$

Referring to the i-vehicle shown in Fig. 2, let $P_0(x_{0i}, y_{0i})$ be the reference point of the motion and indicate the orientation with θ_i. Indicate with (X, Y) and with (X_c, Y_c) the ground and the body references respectively. Let r_i be the radius of the wheels. Indicate with b_i the distance from the center of the wheel to the longitudinal axis and with d_i the distance from the reference point to the mass center P_c. For the later description indicate with m_i and I_i the mass and the inertia of the *i*-vehicle respectively. In view of the previous considerations, the following model can be written:

$$\begin{aligned}
&\dot{\mathbf{q}}_i(t) = \mathbf{S}_i(\mathbf{q}_i(t))\mathbf{v}_i(t), \\
&\mathbf{S}_i(\mathbf{q}_i(t)) = \begin{pmatrix} \cos\theta_i(t) & 0 \\ \sin\theta_i(t) & 0 \\ 0 & 1 \end{pmatrix}, \\
&\mathbf{v}_i^{\mathrm{T}}(t) = \left[u_i(t) \;\; \omega_i(t)\right], \mathbf{q}_i^{\mathrm{T}}(t) = \left[x_{0i}(t) \;\; y_{0i}(t) \;\; \theta_i(t)\right], \\
&i = 1 \ldots r,
\end{aligned} \tag{6}$$

where $u_i(t)$ and $\omega_i(t)$ are the linear and angular velocities of the *i*-cybercar of the cooperative system.

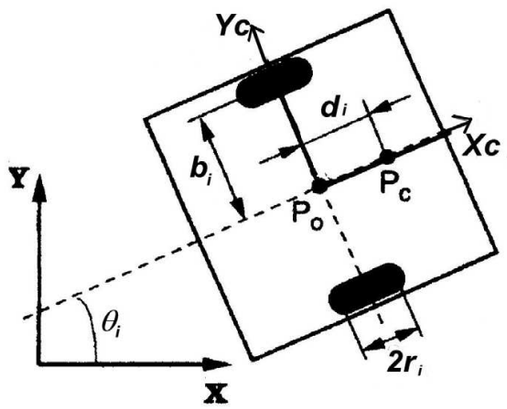

Fig. 2. Cybercar with reference systems

To design a control law which consider the ISO 2631-1, and, therefore, to analyze the vibration of the passengers during the motion, it is necessary to obtain the acceleration model. Let the acceleration vector of each cooperative vehicle be:

$$\begin{aligned}
&\mathbf{a}_{\mathbf{w}i}^{\mathrm{T}}(t) = \left[\hat{a}_{xi}(t) \;\; \hat{a}_{yi}(t)\right] \\
&i = 1, \ldots, r
\end{aligned} \tag{7}$$

The accelerations $\hat{a}_{xi}(t)$ and $\hat{a}_{yi}(t)$ are the *longitudinal and lateral accelerations* respectively of the *i*-cybercar of the cooperative system. The accelerations (7) could be obtained through the following steps. By considering the kinematical model of a non-holonomic vehicle (cf. eq. 6), it is possible to calculate the accelerations along the axes of the ground reference (X,Y) (see Fig. 2) in function of the linear and angular velocities. It results:

$$a_{xi}(t)=\frac{d^2x_{0i}(t)}{dt^2}=\ddot{x}_{0i}(t);$$
$$a_{yi}(t)=\frac{d^2y_{0i}(t)}{dt^2}=\ddot{y}_{0i}(t). \tag{8}$$

Differentiating (6) leads to:

$$\begin{bmatrix}\ddot{x}_{0i}(t)\\ \ddot{y}_{0i}(t)\\ \ddot{\theta}_i(t)\end{bmatrix}=\begin{bmatrix}-\dot{\theta}_i(t)\sin\theta_i(t) & 0\\ \dot{\theta}_i(t)\cos\theta_i(t) & 0\\ 0 & 0\end{bmatrix}\begin{bmatrix}u_i(t)\\ \omega_i(t)\end{bmatrix}+$$
$$+\begin{bmatrix}\cos\theta_i(t) & 0\\ \sin\theta_i(t) & 0\\ 0 & 1\end{bmatrix}\begin{bmatrix}\dot{u}_i(t)\\ \dot{\omega}_i(t)\end{bmatrix}, \tag{9}$$
$$i=1\ldots r.$$

Therefore the human body is subjected to forces along the X and Y axes. Now it is necessary to project the forces above along the axes of the body reference, i.e. X_c and Y_c, so that the lateral and longitudinal accelerations (7) can be calculated as:

$$\hat{a}_{xi}(t)=a_{xi}(t)\cos\theta_i(t)+a_{yi}(t)\cos\theta_i(t);$$
$$\hat{a}_{yi}(t)=a_{yi}(t)\cos\theta_i(t)-a_{xi}(t)\sin\theta_i(t). \tag{10}$$

After some calculations it results:

$$\hat{a}_{xi}(t)=-u_i(t)\dot{\theta}_i(\mathrm{t})\sin\theta_i(t)\cos\theta_i(t)+\dot{u}_i(\mathrm{t})\cos^2\theta_i(t)+$$
$$+u_i(t)\dot{\theta}_i(\mathrm{t})\cos\theta_i(\mathrm{t})\sin\theta_i(t)+\dot{u}_i\sin^2\theta_i(t)=\dot{u}_i;$$
$$\hat{a}_{yi}=-u_i(t)\dot{\theta}_i(t)\sin\theta_i(t)\cos\theta_i(t)+\dot{u}_i(t)\cos^2\theta_i(t)+ \tag{11}$$
$$+u_i(t)\dot{\theta}_i(t)\cos\theta_i(t)\sin\theta_i(t)+\dot{u}_i(t)\sin\theta_i(t)\ =u_i\dot{\theta}_i.$$

Due to non-holonomic constraints given by (2), the components of $\mathbf{q}_i$ (i=1…r) vector are not independent. For this reason the dynamic model (3) cannot be employed directly for the motion control. A dynamic model in body fixed coordinates has to be used. Substituting the equation (6) into model (3) leads to:

$$\overline{\mathbf{M}}_i\dot{\mathbf{v}}_i(t)+\overline{\mathbf{V}}_{\mathbf{m}i}(\omega_i(t))\mathbf{v}_i(t)=\mathbf{S}_i^{\mathrm{T}}(\mathbf{q}_i(t))\mathbf{E}_i(\mathbf{q}_i(t))\boldsymbol{\tau}_i(t) \tag{12}$$
$$i=1\ldots r,$$

where:

$$\overline{\mathbf{M}}_i=\mathbf{S}_i^{\mathrm{T}}(\mathbf{q}_i(t))\mathbf{M}_i(\mathbf{q}_i(t))\mathbf{S}_i(\mathbf{q}_i(t))=\begin{pmatrix}m_i & 0\\ 0 & I_i\end{pmatrix},$$
$$\overline{\mathbf{V}}_{\mathbf{m}i}(\omega_i(t))=\mathbf{S}_i^{\mathrm{T}}(\mathbf{q}_i(t))(\mathbf{M}_i(\mathbf{q}_i(t))\dot{\mathbf{S}}_i(\mathbf{q}_i(t))+\mathbf{V}_{\mathbf{m}i}(\mathbf{q}_i(t))\mathbf{S}_i(\mathbf{q}_i(t)))=\begin{pmatrix}0 & -d_i\omega_i m_i\\ d_i\omega_i m_i & 0\end{pmatrix}, \tag{13}$$
$$i=1\ldots r.$$

3. Decentralized cooperative trajectory planning algorithm

In this paragraph a new decentralized trajectory planning algorithm is developed for the non-holonomic cooperative motion of the cybercars. The problem is the following. All the cybercars must reach a target position without collisions between them. Once the distances between the initial positions of the cybercars and the target are known, a decentralized algorithm permits to plane circular trajectories intersection-free. After communication to each cybercar of the initial position and target coordinates, the trajectory planner of each cybercar provide to plane a circular trajectory independently of each other. This means we have a decentralized planner. More precisely, indicate with $[x_{0i}(0) \quad y_{0i}(0) \quad \theta_i(0)]$ the initial position and orientation of each cybercar. An automated vehicle moving with constant linear and angular velocities, tracks a circular trajectory. Therefore a reference motion may be planned along a circumference that includes the initial coordinates above and the position of the target. With reference to Fig. 3, let $C_i(x_{oi}(0), y_{0i}(0), \theta_i(0)$ be the initial position of the i-cybercar. Let $B(x_T, y_T, \theta_T)$ the position and orientation of the target. Let Δx_i and Δy_i be the shiftings along the tangent and radial directions respectively of the i-vehicle. The i-cybercar moves from C_i to B along a circular trajectory of which the radius is equal to λ_i, while the center is located in D.

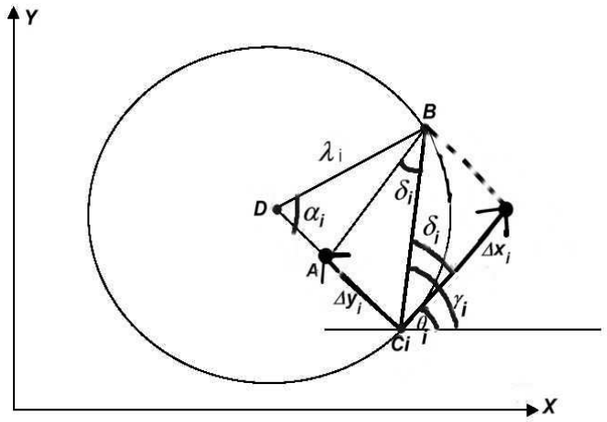

Fig. 3. Motion planning

It yields:

$$\begin{aligned} BC_i &= \tilde{d}_i = \sqrt{(x_T - x_{0i}(0))^2 + (y_T - y_{0i}(0))^2}, \\ \gamma_i &= \arctan\left[(y_T - y_{0i}(0))/(x_T - x_{0i}(0))\right], \\ i &= 1...r, \end{aligned} \tag{14}$$

where γ_i is the angle between BC_i and the *x* axis. Consider the following angular relation (see Fig .3):

$$\begin{aligned} \delta_i &= \gamma_i - \theta_i(0) = \\ &= \arctan\left[(y_T - y_{0i}(0))/(x_T - x_{0i}(0))\right] - \theta_i(0). \end{aligned} \tag{15}$$

The length of the line BA is equal to the distance Δx_i. Therefore, if we consider the triangle $C_i AB$, then:

$$\Delta x_i = \tilde{d}_i \cos\delta_i;\ \Delta y_i = \tilde{d}_i \sin\delta_i. \tag{16}$$

The angular shifting α_i between C_i and B results as it follows:

$$\Delta x_i = \lambda_i \sin\alpha_i. \tag{17}$$

From observation of the triangle DAB, it results:

$$\lambda_i^2 = (\lambda_i - \Delta y_i)^2 + \Delta^2 x_i. \tag{18}$$

The solution of the equation (13) with respect to λ_i is:

$$\lambda_i = (\Delta^2 x_i + \Delta^2 y_i)/2\Delta y_i. \tag{19}$$

Now the values of the reference angular (ω_{ri}) and linear (u_{ri}) velocities of each cooperative vehicle may be calculated as follows:

$$\omega_{ri} = \frac{\alpha_i}{\Delta T};\ u_{ri} = \omega_i \lambda_i;\quad i = 1...r, \tag{20}$$

where ΔT is a fixed look-ahead time interval chosen by the designer. Let us consider multiple automated cybercars in an initial open chain configuration (cf. Fig. 1), i.e. collinear and with the same orientations given by Δx_i *(i=1,2)*. The algorithm above allows circular trajectories without intersections to be planned, so that the vehicles will avoid collisions while moving. Each trajectory is planned independently of the others. This means we have a decentralized cooperation of the vehicles. Fig. 4 shows an example, where two vehicles are considered in open chain configuration $C_1 - C_2$. One observes that the first vehicle of the open chain follows a circular trajectory from C_1 to the target *B* along Δx_1, while the second vehicle follows a circular trajectory from C_2 to the target one along Δx_2. The distance between C_1 and B is smaller than the distance between C_2 and *B*, so that, based on the equation (9), it is $\tilde{d}_1 < \tilde{d}_2$. Consequently, based on the equations (16) and (19), the radius of the circumference tracked by the first vehicle (i.e. λ_1) is smaller than the radius of the circumference tracked by the second vehicle (i.e. λ_2). Since the cybercars are initially collinear and have the same orientations, and the circumferences must be include both the initial positions of the vehicles and the target position, the trajectories are without intersections and the vehicles can reach the target without collisions. The method can be used for *r* cooperative vehicles in initial open chain $C_1 - C_2 - ... - C_r$, so that each vehicle can reach the target without coming into collision with other vehicles.

Note that the vehicles have to be in open chain configuration initially, i.e. collinear. If there is a vehicle which is not mutually collinear, it must reach a collinear position. On this subject, some studies have focused on modelling formations of non-holonomic vehicles (Bicho & Monteiro, 2003).

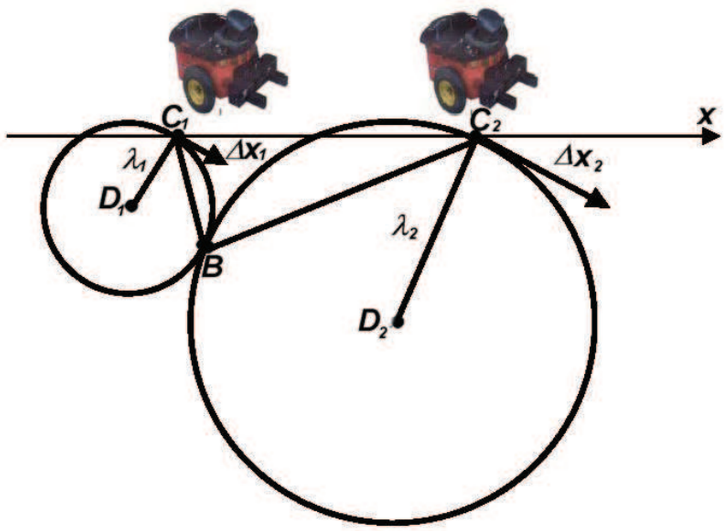

Fig. 4. Trajectory planning without collisions for multiple vehicles in initial open chain configuration

4. Fuzzy dynamic closed loop motion control for cooperative cybercars with passengers comfort

Consider the *i*-cybercar of the cooperative system (cf. Fig. 2).The kinematical model is given by (6), while the dynamical model is given by (12) and (13). Employing the values of linear and angular velocities given by (20) and using the kinematical model (6) lead to the following equations for the circular reference motion of each cybercar:

$$\begin{aligned} &\dot{x}_{r\,i}(t) = u_{ri}\cos\theta_{ri}(t); \dot{y}_{ri}(t) = u_{ri}\sin\theta_{ri}(t); \\ &\dot{\theta}_{ri}(t) = \omega_{ri}, \quad i = 1...r. \end{aligned} \tag{21}$$

Let the following vectors:

$$\begin{aligned} &\mathbf{q}_i^{\mathrm{T}}(t) = \left[x_{0i}(t) \;\; y_{0i}(t) \;\; \theta_i(t)\right], \\ &i = 1...r \end{aligned} \tag{22}$$

be the position and orientation of each cybercar. One defines the following motion errors between the planned circular reference trajectories the state variables given by (22) as it follows:

$$\mathbf{e}_i(t) = \begin{bmatrix} \cos\theta_i(t) & \sin\theta_i(t) & 0 \\ -\sin\theta_i(t) & \cos\theta_i(t) & 0 \\ 0 & 0 & 1 \end{bmatrix} \times \begin{bmatrix} x_{ri}(t) - x_{0i}(t) \\ y_{ri}(t) - y_{0i}(t) \\ \theta_{ri}(t) - \theta_i(t) \end{bmatrix} = \begin{bmatrix} e_{xi}(t) \\ e_{yi}(t) \\ e_{\theta\,i}(t) \end{bmatrix}, \quad i = 1...r. \tag{23}$$

The errors $e_{xi}(t)$ and $e_{yi}(t)$ are said to be the longitudinal and lateral motion errors respectively, while $e_{\theta i}(t)$ is the orientation error. The following velocity control laws are employed for each cybercar:

$$\mathbf{v}_{ci}(t)=\begin{bmatrix} u_{ci}(t) \\ \omega_{ci}(t) \end{bmatrix}=\begin{bmatrix} u_{ri}\cos e_{\theta i}(t)+K_{1i}e_{xi}(t) \\ \omega_{ri}+u_{ri}(K_{2i}e_{yi}(t)+K_{3i}\sin e_{\theta i}(t)) \end{bmatrix},$$
$$K_{1i},K_{2i},K_{3i}>0, \qquad (24)$$
$$i=1\ldots r.$$

Replacing (24) into (6) leads to the following closed loop mathematical model:

$$\dot{\mathbf{e}}_i(t)=\begin{bmatrix} (\omega_{ri}+u_{ri}(K_{2i}e_{yi}(t)+K_{3i}\sin e_{\theta i}(t)))e_{yi}(t)-K_{1i}e_{xi}(t) \\ -(\omega_{ri}+u_{ri}(K_{2i}e_{yi}(t)+K_{3i}\sin e_{\theta i}(t)))e_{xi}(t)+u_i\sin e_{\theta i}(t) \\ -u_{ri}(K_{2i}e_{yi}(t)+K_{3i}\sin e_{\theta i}(t)) \end{bmatrix}, \qquad (25)$$
$$i=1\ldots r.$$

It is possible to formulate the following theorem.

Theorem 1. Consider the cooperative system (6), in closed loop with the velocity control laws (24). If the linear and angular reference velocities given by (21) are limited functions, then the equilibrium state of the closed loop model (25) is the origin of the state space and it is asymptotically stable.

Proof. From model (25), it is evident that, if $\dot{\mathbf{e}}_i(t)=0$ (*i=1…r*), then $\mathbf{e}_i(t)=0$ (*i=1…r*), so that the equilibrium point is the origin of the state space. Consider the following extended vector $\mathbf{e}(t)\in R^{(r\times n)\times 1}$ which contains the motion errors of all the cooperative vehicles:

$$\mathbf{e}^{\mathbf{T}}(t)=\left[\mathbf{e}_1(t)\ \ \mathbf{e}_2(t)\ \ .\ \ .\ \ .\ \ \mathbf{e}_r(t)\right]. \qquad (26)$$

The following Lyapunov's function is chosen:

$$V(\mathbf{e}(t))=\frac{1}{2}\sum_{i=1}^{r}K_{1i}(e_{xi}^2(t)+e_{yi}^2(t))+2\sum_{i=1}^{r}\frac{K_{1i}}{K_{2i}}(1-\cos e_{\theta i}(t)). \qquad (27)$$

The function (27) is definite positive. By calculating the time derivative of the function (27) and substituting the equations (25) into result, it yields:

$$\dot{V}(\mathbf{e}(t))=-\sum_{i=1}^{r}K_{1i}e_{xi}^2(t)-\sum_{i=1}^{r}u_{ri}\frac{2K_{1i}K_{3i}}{K_{2i}}\sin^2 e_{\theta i}(t). \qquad (28)$$

The function (28) does not depend on lateral motion errors $e_{yi}(t)$ (*i=1…r*), so that it is equal to zero in correspondence of the inputs $\left[\ 0\ \ e_{yi}(t)\ \ 0\ \right]$. Therefore the function (28) is semi-definite negative. The conclusion is that the components of the vector (26) are stable and bounded. Since all the motion errors and the reference velocities are bounded, the second time derivative of the function (28) is bounded, therefore Barbalat's lemma implies that the function (28) converges to zero when *t* diverges, so that the longitudinal motion errors and the orientation errors of all the cooperative vehicles converge to zero. From the second and third equations of system (20) it follows that:

$$\lim_{t\to\infty} \dot{e}_{yi}(t) = 0, \quad i = 1 \ldots r. \tag{29}$$

Therefore:

$$e_{yi}(\infty) = \bar{e}_{yi}, \quad i = 1 \ldots r. \tag{30}$$

where $\bar{e}_{yi}$ is a constant value. Since the orientation errors converge to zero, from the third equation of the system (25) it results:

$$-u_i K_{2i} \bar{e}_{yi} = 0, \quad i = 1 \ldots r. \tag{31}$$

It can be concluded that the lateral motion errors converge asymptotically to zero. Q.E.D.
By employing the kinematical control strategy (24), it is difficult to control directly the lateral and longitudinal accelerations which are responsible of harmful effects on the passengers. For this reason a fuzzy dynamical control strategy is developed below, where the properties of the fuzzy maps assures the Lyapunov's stability of the motion errors given by (25), while the saturation properties of the maps ones permit to control directly the maximum acceleration of each vehicle of the cooperative system during the motion. Let $\tilde{\boldsymbol{\eta}}_i(t)$ the time varying error between the velocity control laws given by (24) and the physical velocity $\mathbf{v}_i(t)$ of each cybercar (i.e. the solution of the differential equations (12)):

$$\tilde{\boldsymbol{\eta}}_i(t) = \begin{bmatrix} \tilde{\eta}_{1i}(t) \\ \tilde{\eta}_{2i}(t) \end{bmatrix} = [\mathbf{v}_{ci}(t) - \mathbf{v}_i(t)], \quad i = 1 \ldots . r. \tag{32}$$

The fuzzy inference mechanism is explained below. The inputs of the fuzzy system are the errors (32). The fuzzy rules for $\tilde{\eta}_{ji}$ (*j=1,2* and *i=1,2…r*) are the following:

1) if $\tilde{\eta}_{ji}$ is negative and $\dot{\tilde{\eta}}_{ji}$ is negative then the output Σ_{ji} has a negative big value;

2) if $\tilde{\eta}_{ji}$ is negative and $\dot{\tilde{\eta}}_{ji}$ is positive, then the output Σ_{ji} has a negative small value;

3) if $\tilde{\eta}_{ji}$ is positive and $\dot{\tilde{\eta}}_{ji}$ is negative, then the output Σ_{ji} has a positive small value;

4) if $\tilde{\eta}_{ji}$ is positive and $\dot{\tilde{\eta}}_{ji}$ is positive, then the output Σ_{ji} has a positive big value.

Now we assume the following dynamical control laws (Raimondi & Melluso, 2007-b):

$$\begin{aligned} &\mathbf{S}_i^T(\mathbf{q}_i(t))\mathbf{E}_i(\mathbf{q}_i(t))\boldsymbol{\tau}_i(t) = \\ &= \overline{\mathbf{M}}_i(\dot{\mathbf{v}}_{ci}(t) + \dot{\mathbf{s}}_i(t)) + \overline{\mathbf{V}}_{mi}(\omega_i(t))\mathbf{v}_i(t) = \begin{bmatrix} F_i(t) \\ T_i(t) \end{bmatrix}, \\ &i = i \ldots r \end{aligned} \tag{33}$$

where $\mathbf{S}_i(\mathbf{q}_i(t))$, $\overline{\mathbf{M}}_i$ and $\overline{\mathbf{V}}_{\mathbf{m}i}(\omega_i(t))$ are given by (6) and (13) respectively, $F_i(t)$ and $T_i(t)$ are the linear force and the angular momentum applied to the *i*-cybercar, while $\dot{\mathbf{s}}_i(t)$ is the output of the fuzzy inference system, so that it is:

$$\dot{\mathbf{s}}_i(t) = \mathbf{\Sigma}_i(\tilde{\boldsymbol{\eta}}_i(t), \dot{\tilde{\boldsymbol{\eta}}}_i(t)) = \begin{bmatrix} \Sigma_{1i}(\tilde{\eta}_{1i}(t), \dot{\tilde{\eta}}_{1i}(t)) \\ \Sigma_{2i}(\tilde{\eta}_{2i}(t), \dot{\tilde{\eta}}_{2i}(t)) \end{bmatrix}, \quad i = 1...r \tag{34}$$

where $\mathbf{\Sigma}_{ji}$ (*j=1,2 i=1…r*) are the nonlinear input-output maps of the fuzzy inference system. The maps above depends on the choice of the input and output memberships. Figs 5 and 6 show the membership functions for obtaining Σ_{1i} (*i=1…r*).

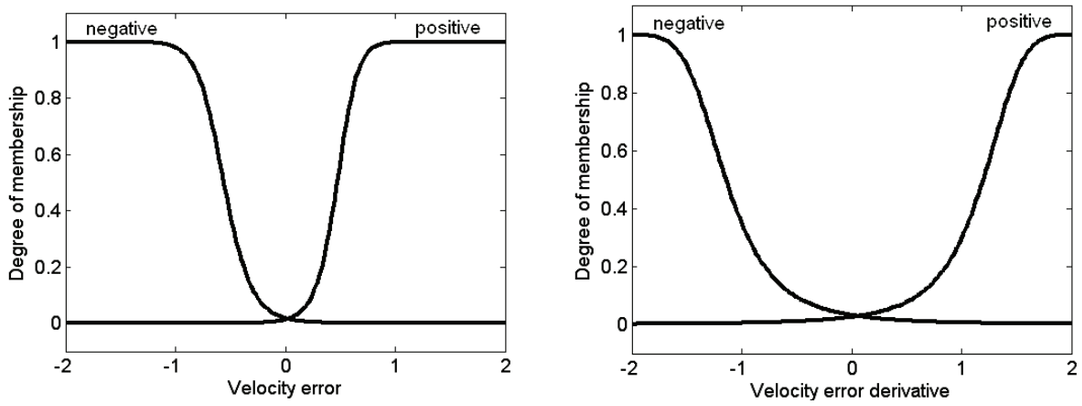

Fig. 5. Input membership functions

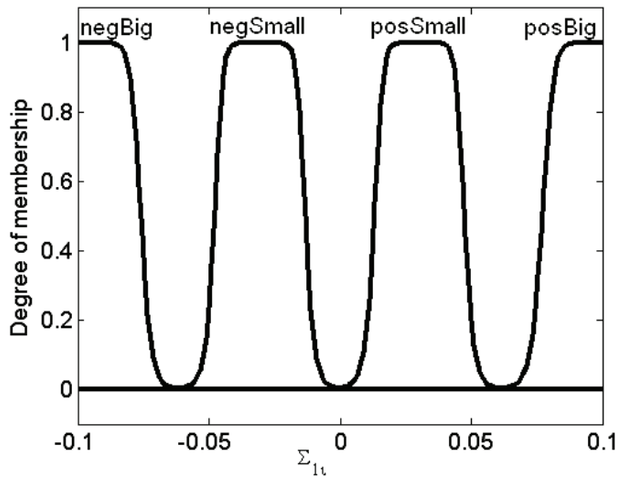

Fig. 6. Output membership function

The memberships employed for obtaining the control surfaces Σ_{2i} (*i=1…r*) have the same symmetry. The input values of the memberships of Fig. 5 are chosen in such a way to be in the range of the physical velocity errors obtained in our application. The outputs Σ_{ji} (*j=1,2*

i=1,2,…r) given by (34) represent the variations of the torques applied to the right and left wheels of each cooperative cybercar for positive or negative changes of the speed errors given by (32). Due to the choice of the form of the memberships functions, the outputs above are nonlinear uniformly continuous and bounded functions. They contribute to evaluating the acceleration or deceleration of the cybercars, to track the planned reference motion with good dynamic perfomances.

Assumption 1. The following properties for the nonlinear fuzzy maps given by (33) are assumed:

$$
\begin{aligned}
&1)\ \Sigma_{ji}(0,0)=0;\\
&2)\ \Sigma_{ji}(\eta_{ji}(t),\dot{\tilde{\eta}}_{ji}(t))=-\Sigma_{ji}(-\tilde{\eta}_{ji}(t),-\dot{\tilde{\eta}}_{ji}(t));\\
&3)\ \exists\delta_{ji}>0:\left|\Sigma_{ji}(\eta_{ji}(t),\dot{\tilde{\eta}}_{ji}(t))\right|\le\delta_{ji};\\
&4)\ \Sigma_{ji}(\eta_{ji}(t),0)=0\Rightarrow\tilde{\eta}_{ji}(t)=0;\\
&5)\ \tilde{\eta}_{ji}(t)\Sigma_{ji}(\tilde{\eta}_{ji}(t),\dot{\tilde{\eta}}_{ji}(t))>0;\\
&6)\ \begin{array}{l}0\le\tilde{\eta}_{ji}(t)(\Sigma_{ji}(\eta_{ji}(t),\dot{\tilde{\eta}}_{ji}(t))-\Sigma_{ji}(0,\dot{\tilde{\eta}}_{ji}(t)));\\ 0\le\dot{\tilde{\eta}}_{ji}(t)(\Sigma_{ji}(\eta_{ji}(t),\dot{\tilde{\eta}}_{ji}(t))-\Sigma_{ji}(\tilde{\eta}_{ji}(t),0)).\end{array}
\end{aligned}
\tag{35}
$$

The assumption above is a necessary condition to ensure that each cooperative cybercar can follow the planned trajectory; also by varying the values δ_{ij}, the acceleration saturation values can be changed, so that the motion of each cybercar can be controlled with low accelerations. Note that, if we choice different number or form of the membership functions, then the properties given by (35) cannot be guaranteed.

Substituting (33) into dynamical model (12) leads to:

$$
\begin{aligned}
&\dot{\tilde{\boldsymbol{\eta}}}_i(t)+\boldsymbol{\Sigma}_i(\tilde{\boldsymbol{\eta}}_i(t),\dot{\tilde{\boldsymbol{\eta}}}_i(t))=\mathbf{0},\\
&i=1\ldots r.
\end{aligned}
\tag{36}
$$

It can be written:

$$
\begin{aligned}
&\overline{\boldsymbol{\Sigma}}_i(\tilde{\boldsymbol{\eta}}_i(t),\dot{\tilde{\boldsymbol{\eta}}}_i(t))=\mathbf{0},\\
&i=1\ldots r,
\end{aligned}
\tag{37}
$$

so that:

$$
\begin{aligned}
&\dot{\tilde{\boldsymbol{\eta}}}_i(t)=\mathbf{f}_i(\tilde{\boldsymbol{\eta}}_i(t)),\\
&i=1\ldots r.
\end{aligned}
\tag{38}
$$

Considering equations (25) and (38) leads to the following closed loop model of the fuzzy dynamic control system:

$$\dot{\mathbf{e}}_i(t)=\begin{bmatrix}\dot{e}_{xi}(t)\\ \dot{e}_{yi}(t)\\ \dot{e}_{\theta i}(t)\end{bmatrix}=\begin{bmatrix}(\omega_{ri}+u_{ri}(K_{2i}e_{yi}(t)+K_{3i}\sin e_{\theta i}(t)))e_{yi}(t)-K_{1i}e_{xi}(t)\\ -(\omega_{ri}+u_{ri}(K_{2i}e_{yi}(t)+K_{3i}\sin(e_{\theta i})))e_{xi}(t)+u_{ri}\sin e_{\theta i}(t)\\ -u_{ri}(K_{2i}e_{yi}(t)+K_{3i}\sin e_{\theta i}(t))\end{bmatrix},$$

$$\dot{\tilde{\boldsymbol{\eta}}}_i(t)=\mathbf{f}_i(\tilde{\boldsymbol{\eta}}_i(t)), \quad (39)$$

$$i=1\ldots r.$$

Now the following theorem may be formulated.

Theorem 2. Consider the closed loop system given by (39). Under the assumption 1, the equilibrium state of the modeled system is the origin of the state space and it is asymptotically stable.

Proof. Consider the following extended state vector:

$$\bar{\mathbf{e}}(t)=\begin{bmatrix}\bar{\mathbf{e}}_1(t)\\ \bar{\mathbf{e}}_2(t)\\ .\\ .\\ .\\ \bar{\mathbf{e}}_r(t)\end{bmatrix}, \quad (40)$$

where:

$$\bar{\mathbf{e}}_i(t)=\begin{bmatrix}e_{xi}(t)\\ e_{yi}(t)\\ e_{\theta i}(t)\\ \tilde{\eta}_{1i}(t)\\ \tilde{\eta}_{2i}(t)\end{bmatrix}=\begin{bmatrix}\mathbf{e}_i(t)\\ \tilde{\boldsymbol{\eta}}_i(t)\end{bmatrix}, \quad (41)$$

$$i=1\ldots r.$$

From equations (39) it results:

$$\left[\dot{e}_{xi}(t)\,\dot{e}_{yi}(t)\,\dot{e}_{\theta i}(t)\right]^{\mathbf{T}}=\mathbf{0},\quad \forall t;\quad i=1\ldots r, \quad (42)$$

so that:

$$\left[e_{xi}(t)\,e_{yi}(t)e_{\theta i}(t)\right]^{\mathbf{T}}=\mathbf{0},\quad \forall t; i=1\ldots r. \quad (43)$$

Also, if $\dot{\tilde{\boldsymbol{\eta}}}_i(t)=\mathbf{0}$, then:

$$\boldsymbol{\Sigma}_i(\tilde{\boldsymbol{\eta}}_i(t),\mathbf{0})=\mathbf{0},\quad i=1\ldots r, \quad (44)$$

so that, based on the property 4 given in the Assumption 1, it can be said that:

$$\begin{aligned} &\tilde{\boldsymbol{\eta}}_{\,i}(t) = \mathbf{0}, \\ &\forall t, \;\; i = 1...r. \end{aligned} \tag{45}$$

This implies that:

$$\begin{aligned} &\mathbf{0} = \mathbf{f}_i(\mathbf{0}), \\ &i = 1...r. \end{aligned} \tag{46}$$

Therefore the equilibrium point of model (39) is the origin of the state space. The following Lyapunov's function is chosen:

$$\begin{aligned} V(\bar{\mathbf{e}}(t)) = &\frac{1}{2}\sum_{i=1}^{r} K_{1i}(e_{xi}^2(t) + e_{yi}^2(t)) + 2\sum_{i=1}^{r} \frac{K_{1i}}{K_{2i}}(1 - \cos e_{\theta i}(t)) \\ &+ \frac{1}{2}\sum_{i=1}^{r} \tilde{\boldsymbol{\eta}}_i^{\mathrm{T}}(t)\tilde{\boldsymbol{\eta}}_i(t) + + \sum_{j=1}^{2}\sum_{i=1}^{r}\int_0^{\tilde{\eta}_{ji}} \Sigma_{ji}(\xi_{ji}, 0)d\xi_{ji} \;, \\ K_{1i}, K_{2i} > 0. \end{aligned} \tag{47}$$

The first, second and third terms of function (47) are always positive. Now, from the property 6 of the fuzzy maps it results:

$$\begin{aligned} &0 \le \tilde{\eta}_{ji}(t)(\Sigma_{ji}(\eta_{ji}(t), \dot{\tilde{\eta}}_{ji}(t)) - \Sigma_{ji}(0, \dot{\tilde{\eta}}_{ji}(t))), \\ &j = 1,2; \;\; i = 1,2,...r. \end{aligned} \tag{48}$$

Consequently, if $\dot{\eta}_{ji}(t) = 0$, then it yields:

$$0 \le \tilde{\eta}_{ji}(t)(\Sigma_{ji}(\eta_{ji}(t), 0) - \Sigma_{ji}(0,0)), \tag{49}$$

so that, based on the property 1, one obtains:

$$\begin{aligned} &0 \le \tilde{\eta}_{ji}(t)\Sigma_{ji}(\eta_{ji}(t), 0), \\ &j = 1,2; \;\; i = 1,2...r. \end{aligned} \tag{50}$$

It can be concluded that:

$$\begin{aligned} &\sum_{j=1}^{2}\sum_{i=1}^{r}\int_0^{\tilde{\eta}_{ji}} \Sigma_{ji}(\xi_{ji}, 0)d\xi_{ji} > 0, \quad \forall \tilde{\eta}_{ji}, \\ &j = 1,2; \;\; i = 1,2...r. \end{aligned} \tag{51}$$

Therefore the function (47) is positive definite. Calculating the time derivative of the function (47) and replacing (39) into it lead to:

$$\dot{V}(\bar{\mathbf{e}}) = -\sum_{i=1}^{r} K_{1i} e_{xi}^2(t) - \sum_{i=1}^{r} u_{ri} \frac{2K_{1i}K_{3i}}{K_{2i}} \sin^2(e_{\theta i}(t)) - \sum_{i=1}^{r} \tilde{\boldsymbol{\eta}}_i^{\mathrm{T}}(t) \boldsymbol{\Sigma}_i(\tilde{\boldsymbol{\eta}}_i(t), \dot{\tilde{\boldsymbol{\eta}}}_i(t)) + \\ - \sum_{i=1}^{r} \boldsymbol{\Sigma}_i^{\mathrm{T}}(\tilde{\boldsymbol{\eta}}_i(t), \dot{\tilde{\boldsymbol{\eta}}}_i(t)) \boldsymbol{\Sigma}_i(\tilde{\eta}_i(t), \mathbf{0}) \ . \tag{52}$$

The first and second terms of (52) are negative. Based on the property 5 (see Assumption 1), the elements of the summation of the third term of (52) are positive numbers, so that the term above is negative. From property 5 and inequality (50) it yields:

$$\tilde{\eta}_{ji}^2(t) \Sigma_{ji}(\tilde{\eta}_{ji}(t), 0) \Sigma_{ji}(\tilde{\eta}_{ji}(t), \dot{\tilde{\eta}}_{ji}(t)) > 0, \\ j = 1,2; \quad i = 1,2,...,r, \tag{53}$$

so that, if $\Sigma_{ji}(\tilde{\eta}_{ji}(t), 0)$ is positive, then $\Sigma_{ji}(\tilde{\eta}_{ji}(t), \dot{\tilde{\eta}}_{ji}(t))$ is positive. Therefore the elements of the summation of the fourth term of function (52) are positive. Note that function (52) does not depend on the lateral error, therefore it can be concluded that the function above is negative semi-definite. Therefore the components of the vector (40) are bounded. Now it is possible to calculate the second time derivative of function (47). Based on the previous considerations, it is a bounded function, so that, by applying the Barbalat's lemma, it follows that:

$$\lim_{t \to \infty} \dot{V}(\bar{\mathbf{e}}) = 0. \tag{54}$$

From (52) it can be concluded that the errors $e_{xi}, e_{\theta i}, \tilde{\eta}_{1i}, \tilde{\eta}_{2i}$ (*i=1,…,r*) converge to zero. Replacing (24) into (32) leads to:

$$\tilde{\boldsymbol{\eta}}_i(t) = \begin{bmatrix} u_{ci}(t) - u_i(t) \\ \omega_{ci}(t) - \omega_i(t) \end{bmatrix} = \begin{bmatrix} \tilde{\eta}_{1i}(t) \\ \tilde{\eta}_{2i}(t) \end{bmatrix} = \\ = \begin{bmatrix} u_{ri} \cos(e_{\theta i}(t)) + K_{1i} e_{xi}(t) - u_i(t) \\ \omega_{ri} + K_{2i} u_{ri} e_{yi}(t) + K_{3i} u_{ri} \sin e_{\theta i}(t) - \omega_i(t) \end{bmatrix}, \\ i = 1...r. \tag{55}$$

Since the errors $e_{xi}, e_{\theta i}, \tilde{\eta}_{1i}, \tilde{\eta}_{2i}$ converge asymptotically to zero, the lateral errors e_{yi} of each cooperative cybercar converges asymptotically to zero. Q.E.D.

Fig. 7 illustrates the block scheme of the Fuzzy dynamical motion closed loop control system for a single cybercar.

With regards to the passengers comfort, several factor influence vibration discomfort in relation to passenger activities, e.g. seated posture, use of backrest. Passengers usually adopt their posture to attenuate the intensity of vibrations and jerks in order to perform their activities satisfactorily. However the transmission of vibrations on the human body is higher if a passenger uses armrest, backrest or places boot feet on the floor. Therefore attenuation of vibration exposure is a very important requirement of a motion control system for cybercars. There are various means by which the vibration may be expressed, such as

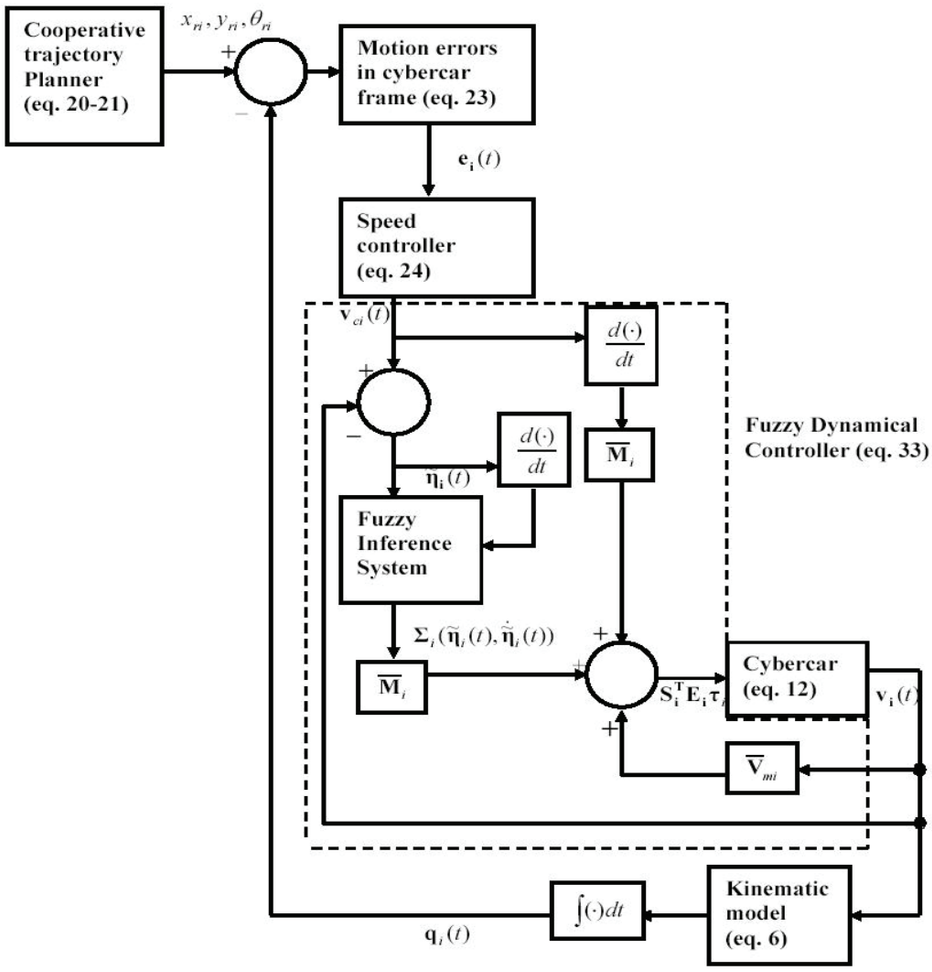

Fig. 7. Block scheme of the dynamical fuzzy control system for cybercar motion

displacement, velocity and acceleration. Of these physical quantities acceleration is generally adopted as preferred measured of quantifying the severity of human vibration exposure (Suzuki, 1998). From (10) it appears that the accelerations which cause vibrations on the human body depend on the curvature of the trajectory. Indicate with $\mathbf{a}_{\mathbf{wi}} \in R^2$ the following vector:

$$\begin{aligned} \mathbf{a}_{\mathbf{wi}}^{\mathbf{T}} &= \left[\hat{a}_{xi}(t)\ \ \hat{a}_{yi}(t)\right], \\ i &= 1 \ldots r, \end{aligned} \tag{56}$$

where $\hat{a}_{xi}(t)$ and $\hat{a}_{yi}(t)$ are the accelerations given by (11). Indicate with $\overline{a}_{xi}$ and $\overline{a}_{yi}$ the r.m.s. values of the accelerations given by (56). Indicate the jerks with the following vector:

$$\begin{aligned} \mathbf{j}_i^{\mathbf{T}}(t) &= [j_{xi}(t)\ \ j_{yi}(t)], \\ i &= 1 \ldots r\,. \end{aligned} \tag{57}$$

The components $j_{xi}(t)$ and $j_{yi}(t)$ are said to be the *lateral and longitudinal jerks* of each cybercar, i.e. the rate of change of the accelerations as it follows:

$$\begin{aligned} j_{xi}(t) &= \frac{d\hat{a}_{xi}(t)}{dt}, \\ j_{yi}(t) &= \frac{d\hat{a}_{yi}(t)}{dt}, \\ i &= 1...r. \end{aligned} \tag{58}$$

Indicate with $\bar{j}_{xi}$ and $\bar{j}_{yi}$ the R.M.S. values of the jerks given by (58). The ISO 2631-1 Standard relates comfort of the passengers with the r.m.s. overall acceleration which causes vibrations acting on the human body defined as:

$$\begin{aligned} \tilde{a}_{wi} &= \sqrt{\alpha^2 \bar{a}_{xi}^{\ 2} + \beta^2 \bar{a}_{yi}^2 + \gamma^2 \bar{a}_{zi}^2}, \\ i &= 1...r, \end{aligned} \tag{59}$$

where $\bar{a}_{xi}$ and $\bar{a}_{yi}$ are given by (56), $\bar{a}_{zi}$ is the acceleration on the *z* axis perpendicular to plane Xc,Yc (see Fig. 2), while α, β and γ are multiplying factors. Since each vehicle moves on the plane, the acceleration $\bar{a}_{zi}$ is equal to zero. Based on the ISO 2631-1, the relations between the values of the overall acceleration given by (58) and the passenger comfort of the *i*-cybercar are given by the Table 1 .

R.M.S. overall acceleration	*Passenger comfort level*
$\tilde{a}_{wi} < 0.315 m/s^2$	Not uncomfortable
$0.315 < \tilde{a}_{wi} < 0.63 m/s^2$	A little uncomfortable
$0.5 < \tilde{a}_{wi} < 1 m/s^2$	Fairy uncomfortable
$0.8 < \tilde{a}_{wi} < 1.6 m/s^2$	Uncomfortable
$1.25 < \tilde{a}_{wi} < 2.5 m/s^2$	Very uncomfortable
$\tilde{a}_{wi} > 2.5 m/s^2$	Extremely uncomfortable

Table 1. ISO 2631-1 Standard

By using our fuzzy approach, it is possible to obtain low values of the lateral and longitudinal accelerations in easy way. In fact the saturation values of the outputs of the fuzzy maps, i.e. the values δ_{ji} given by the third property of (35), represent a saturation of the linear and angular accelerations of the cooperative cybercars, so that they are degree of freedom and can be chosen by the designer. In particular, from equation (9) it can be seen that the accelerations along the axes of the ground reference depend on the linear

acceleration $\dot{u}_i(t)$ and on the angular acceleration $\dot{\omega}_i(t)$. Now, during the motion, the values of $\dot{u}_i(t)$ and $\dot{\omega}_i(t)$ depend on the outputs of the dynamical fuzzy control law given by (33) and (34). Fig. 8 shows the typical fuzzy control surfaces obtained by using the fuzzy control law (33), where the acceleration given by (34) satisfies the properties of the assumption 1.

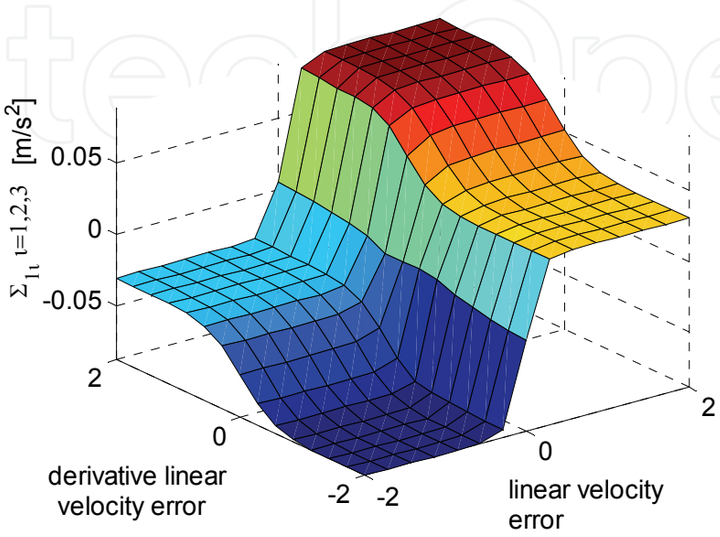

Fig. 8. Fuzzy mapping

The saturation property of the fuzzy map causes the accelerations above to be bounded, and so, after a few attempts, the designer can choose the ranges of the crisp output values of the fuzzy system in order to satisfy the ISO 2631-1 standard and to reduce the vibrations and the jerks. It is evident that the the output values of Fig. 8 fall within a small range, since a motion with low acceleration and jerk is desired. The simulation experiments described in the next section confirm the efficiency of our algorithm in terms of cooperation, stability of the fuzzy motion control system and passenger comfort.

5. Simulation experiments

In this performed simulations the efficiency of the cooperative fuzzy motion control law proposed and developed in this chapter and the good level comfort of the passengers during the motion of the cybercar is illustrated. The parameters of the cybercars have been chosen based on existing cybercars (McDonald & Voge, 2003). The weight of a cybercar is 300kg, the width is 1.45m, the height is 1.6m, while the length is 3.7m. Referring to Fig. 2, the kinematical parameters are chosen as:

$$r_i = 0.40m;\ b_i = 0.725m;\ i = 1,2,3. \tag{60}$$

The dynamical parameters are:

$$M_i = 300kg;\ d_i = 1.5m;\ i = 1,2,3. \tag{61}$$

The parameters of the speed control law (24) are given by:

$$K_{1i} = 25; K_{2i} = 20; \\ i = 1,2,3. \tag{62}$$

The reference trajectories of each cybercar were generated using the decentralized algorithm developed in Section 3, so that the initial motion error values are equal to zero. In fact the circumferences have been generated based on the distance between the initial position of the cybercars and the position of the target. Initially the vehicles are in open chain configuration along y-direction. The initial positions of the three cooperative cybercars are the following:

$$x_{01}(t=0) = 2m;\ x_{02}(t=0) = 2m;\ x_{03}(t=0) = 2m; \\ y_{01}(t=0) = 2m; y_{02}(t=0) = 3m; y_{03}(t=0) = 4m; \\ \theta_{01}(t=0) = 1{,}74rad; \theta_{02}(t=0) = 1.74rad; \theta_{03}(t=0) = 1.74rad. \tag{63}$$

All the generalized coordinates given by (63) refer to a ground reference whose origin is shown in Fig. 9. The position coordinates of the target with respect to the ground reference are:

$$\begin{bmatrix} x_T \\ y_T \end{bmatrix} = \begin{bmatrix} 1.7m \\ -2.8m \end{bmatrix}. \tag{64}$$

To analyze the performances in terms of passenger comforts, we compare for cases with reference to the parameters δ_{ij} given by the third property of (35) :

a. low values of the parameters $\delta_{ji}\ \ (i = 1,2;\ j = 1,2,3)$;

b. high values of the parameters $\delta_{ji}\ \ (i = 1,2;\ j = 1,2,3)$.

Case a- The absolute saturation values of the crisp outputs of the fuzzy control surfaces are:

$$\delta_{1i} = \left|\Sigma_{1i\_sat}\right| = 0.1m/s^2; \\ \delta_{2i} = \left|\Sigma_{2i\_sat}\right| = 0.1rad/s^2; \\ i = 1,2,3. \tag{65}$$

Fig. 9 shows the planar trajectories of the cybercars as planned by using the algorithm given in Section 3.

Initially the cybercars are in open chain configuration. The trajectories are intersections-free and therefore there are not collisions during the motion.

The graphs of Fig. 10 and 11 show the time evolutions of the velocity errors given by (32). Due to the dynamics of the cybercars, there are not perfect velocity tracking, i.e. the speed control laws (24) do not affect instantaneously the linear and angular velocities, but the errors converge to zero after some times.

The most significant graphs which illustrate the stability performances of the motion errors of each cybercar are drawn in Figs. 12 and 13, where the time evolutions of the longitudinal, lateral and orientation errors given by (23) are shown.

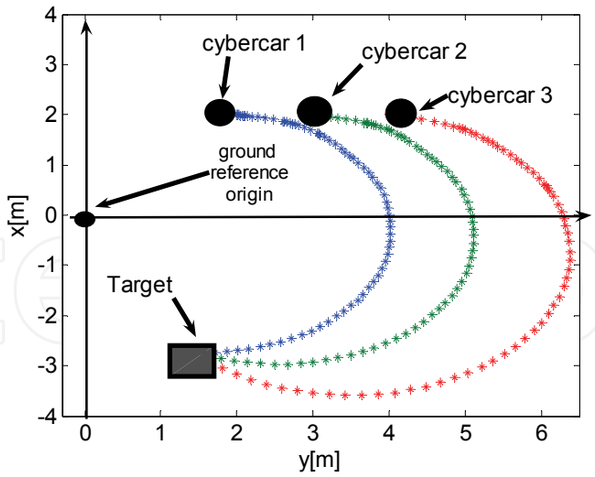

Fig. 9. Motion of three cooperative cybercars

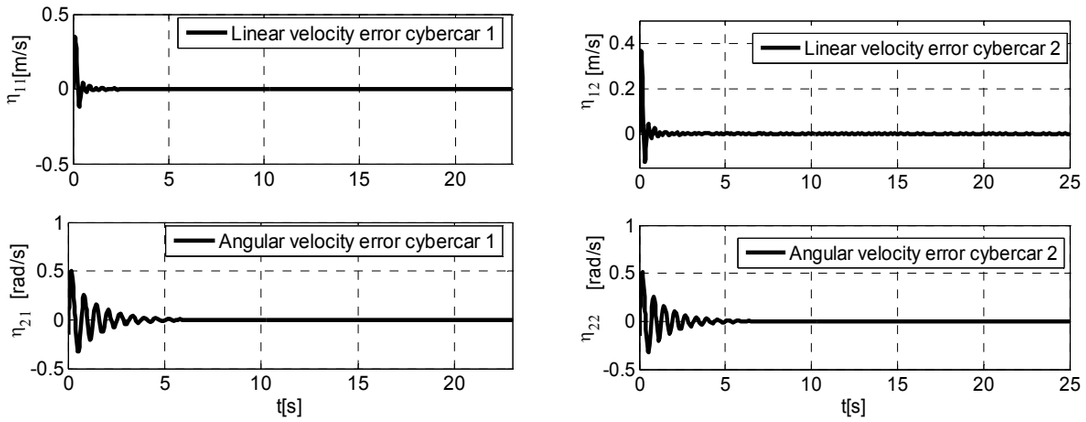

Fig. 10. Velocity errors of the cybercars 1 and 2

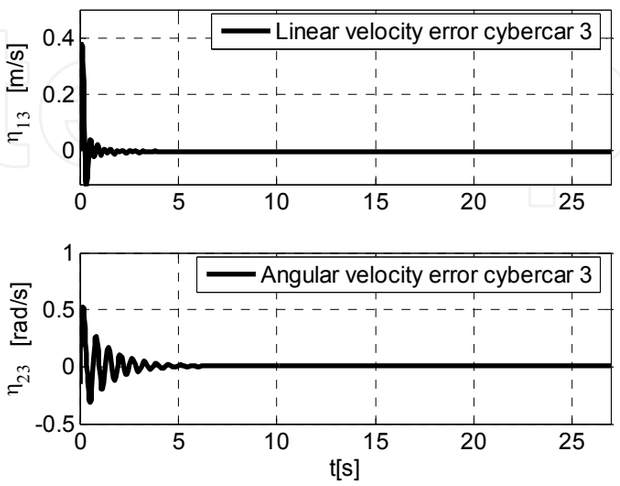

Fig. 11. Velocity errors of the cybercars 3

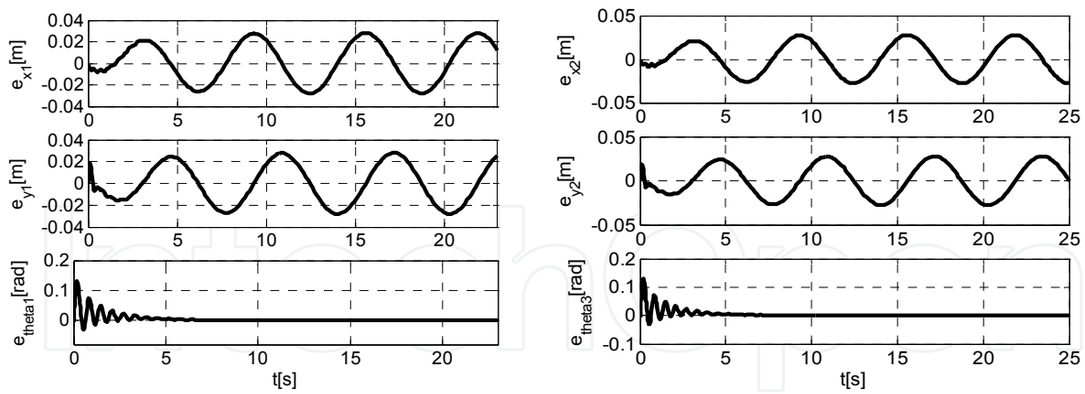

Fig. 12. Tracking errors of cybercars 1 and 2.

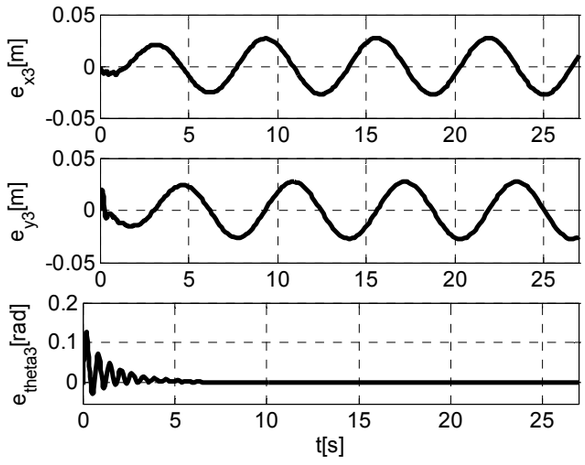

Fig. 13. Tracking errors of cybercar 3

Now we investigate on the passenger comforts with the saturation values given by (65). Figs. 14 and 15 shows the time evolution of the accelerations given by (56) which are responsible of vibrations on the human body, while Table 2 illustrates the r.m.s values of the same accelerations and the overall acceleration given by the mean index (59).

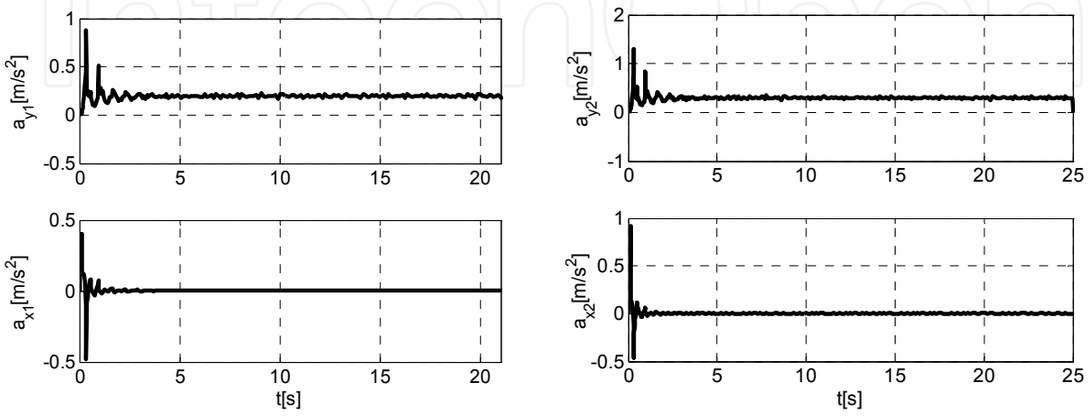

Fig. 14. Lateral and longitudinal accelerations of the cybercars 1 and 2.

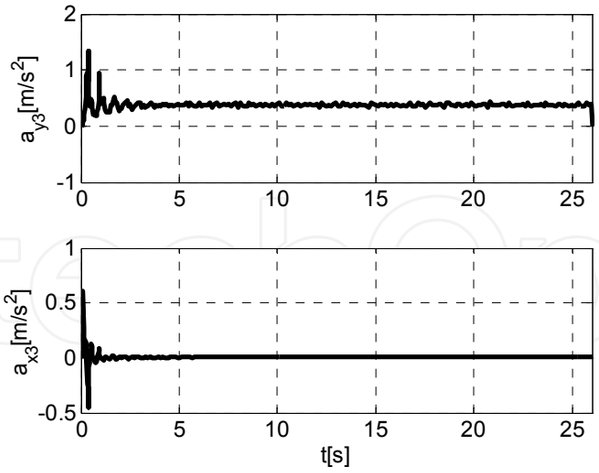

Fig. 15. Lateral and longitudinal accelerations of the cybercars 3.

Longitudinal acceleration	**Lateral acceleration**	**Overall Acceleration**
$\overline{a}_{x1} = 0.0787 m/s^2$	$\overline{a}_{y1} = 0.2034 m/s^2$	$\widetilde{a}_{w1} = 0.305 m/s^2$
$\overline{a}_{x2} = 0.0882\, m/s^2$	$\overline{a}_{y2} = 0.3097 m/s^2$	$\widetilde{a}_{w2} = 0.45 m/s^2$
$\overline{a}_{x3} = 0.0902 m/s^2$	$\overline{a}_{y3} = 0.3853 m/s^2$	$\widetilde{a}_{w3} = 0.554 m/s^2$

Table 2. r.m.s. and mean accelerations of all the cybercars

Note that the values of the r.m.s. overall accelerations are between "Not uncomfortable" and "A little uncomfortable" (see Table 1 and 2), so that the passengers comfort level is very good.

Case b- With respect to (65), the saturation values of the fuzzy control surfaces are increased as follows:

$$\begin{aligned} &\delta_{1i} = \left|\Sigma_{1i\_sat}\right| = 0.5 m/s^2; \\ &\delta_{2i} = \left|\Sigma_{2i\_sat}\right| = 0.5 rad/s^2; \\ &i = 1,2,3. \end{aligned} \tag{66}$$

The comfort of the passengers are also studied in this case. On this subject Figs. 16 and 17 illustrate the lateral and longitudinal accelerations of the cybercars. The r.m.s values of the accelerations above and the mean acceleration given by the index (59) are listed in Table 3, while the values of the jerks given by (58) in cases of low and high saturation values of the fuzzy control surfaces are illustrated in table 4.

Figures 16 and 17 and the results of the table 3 show that the overall accelerations are between "fairy uncomfortable" and "uncomfortable", so that the comfort of the passengers during the motion is bad. By the results shown in Tables 2-4 it is evident that, in case of low

values saturation of the fuzzy control surfaces, the accelerations and the jerks are reduced, which means ride passengers comfort enhancement. Therefore the designer can be choice the parameters of the fuzzy controller to optimize the vibrations acting on the human body of the passengers.

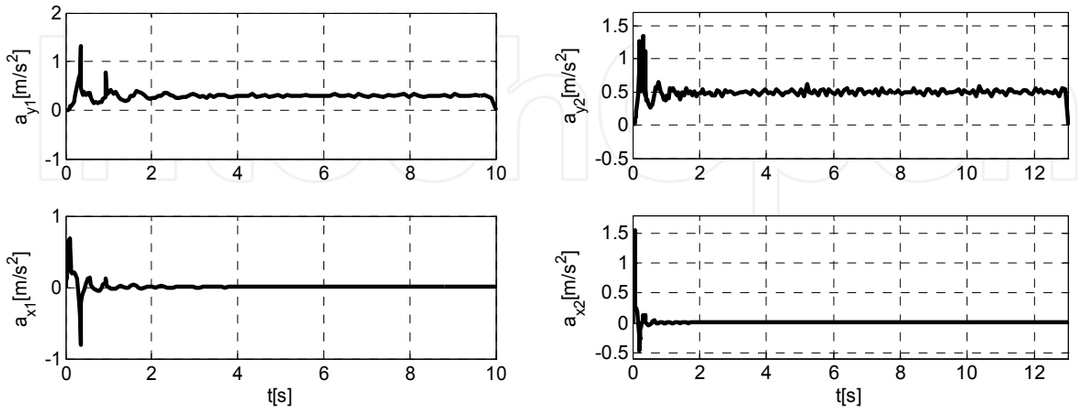

Fig. 16. Lateral and longitudinal accelerations of the cybercars 1 and 2

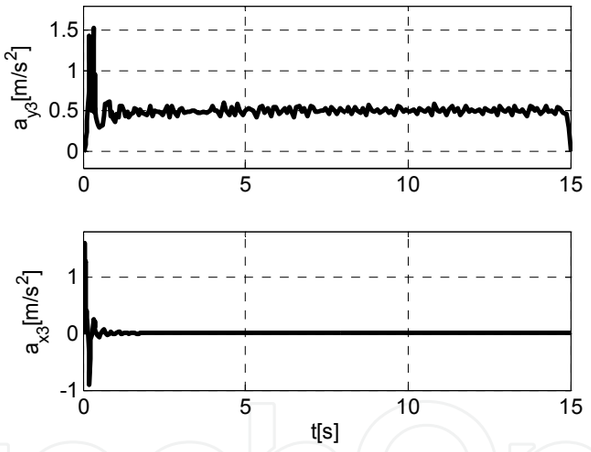

Fig. 17. Lateral and longitudinal accelerations of the cybercar 3

Longitudinal acceleration	Lateral acceleration	Overall Acceleration
$\overline{a}_{x1} = 0.1714 m/s^2$	$\overline{a}_{y1} = 0.3113 m/s^2$	$\widetilde{a}_{w1} = 0.497 m/s^2$
$\overline{a}_{x2} = 0.1903\, m/s^2$	$\overline{a}_{y2} = 0.4934 m/s^2$	$\widetilde{a}_{w2} = 0.54 m/s^2$
$\overline{a}_{x3} = 0.4559\, m/s^2$	$\overline{a}_{y3} = 0.5673 m/s^2$	$\widetilde{a}_{w3} = 0.79 m/s^2$

Table 3. r.m.s. and mean accelerations of all the cybercars

Jerks with low saturation values of the fuzzy control surfaces (cfr. (65)).	Jerks with high saturation values of the fuzzy control surfaces (cfr. (66)).
$\bar{j}_{x1} = 0.1177 m/s^3$	$\bar{j}_{x1} = 1.1589 m/s^3$
$\bar{j}_{y1} = 0.0226 m/s^3$	$\bar{j}_{y1} = 0.4712 m/s^3$
$\bar{j}_{x2} = 0.0458 m/s^3$	$\bar{j}_{x2} = 2.6166 m/s^3$
$\bar{j}_{y2} = 0.0225 m/s^3$	$\bar{j}_{y2} = 0.5837 m/s^3$
$\bar{j}_{x3} = 0.1118 m/s^3$	$\bar{j}_{x3} = 2.2999 m/s^3$
$\bar{j}_{y3} = 0.0226 m/s^3$	$\bar{j}_{y3} = 0.5702 m/s^3$

Table 4. r.m.s. lateral and longitudinal jerks of all the cybercars

6. Conclusion

In this chapter a new fuzzy cooperative control algorithm for multiple fully automated cybercars, where the parameters of fuzzy controller may be tuned to obtain low vibrations on the body of the passengers, has been developed. A generalized mathematical model for multiple cybercars to project the fuzzy control system and an acceleration model to ensure the comfort of the passengers have been formulated. A new decentralized trajectory planner which guarantee the absence of collisions between the closest vehicles has been presented. A new fuzzy control strategy which stabilizes all the cooperative vehicles in the planned trajectories has been developed, where the asymptotical stability of the motion errors has been proved by using Lyapunov's theorem and Barbalat's lemma. Good passengers comfort levels during the motion has been ensured by tuning of the saturation of the fuzzy maps. In the simulation tests an example in case of motion control of three automated vehicles has been developed. Trajectories without intersections have been generated and, by choosing suitable input-output values of the fuzzy maps, the stability of the motion errors and very good passengers comfort levels based on ISO 2631-1 Standard have been obtained.

7. Aknowledgements

This work was realized with the contribution of the MIUR ex-60%.
All sections have been equally and jointly developed by the authors.

8. References

Antonelli, G. & Chiaverini, S. (2006). Kinematic Control of Platoons of Autonomous Vehicles. *IEEE Transactions on Robotics*, Vol. 22, Issue 6, pp. 1285-1292, ISSN 1552-3098.

Bicho, E. & Monteiro, S. (2003). Formation control of multiple mobile robots: a non-linear attractor dynamics approach, *Proceedings of IEEE International Conference on Intelligent Robots and Systems,* pp. 2016-2022, Vol. 2, ISBN 0-7803-7860-1.

Birlik, G. & Sezgin, O. C. (2007). Effect of Vibration on Trasportation System, In: *Springer Proceedings in Physics,* pp. 85-90, Springer Netherlands, ISBN 978-1-4020-5400-6.

Bloch, A.M. (2000). *Nonholonomic Mechanics and Control*, Springer Verlag, ISBN 0-387-95535-6.

Driessen, J.B.; Feddema, J.T. & Kwok, K.S. (1999). Decentralized Fuzzy Control of Multiple Nonholonomic Vehicles. *Journal of Intelligent and Robotic Systems,* Vol. 26, Issue 1, Kluwer Academics Publishers, pp. 65-70, ISSN 0921-0296.

Fierro, R. & Lewis J. (1997). Control of a Nonholonomic Mobile Robots: Backstepping Kinematics into Dynamics. *Journal of Robotics System,* Vol. 14, Issue 3, pp. 149-163, ISSN 0741-2223.

Gerkey, B.P. & Mataric, M.J. (2002). Sold!: Auction Methods for Multi-Robots Coordination. *IEEE Transactions on Robotics and Automation*, Vol. 18, Issue 5, pp. 758-768, ISSN 0882-4967.

La Valle, S.M. & Hutchinson, S.A. (1998). Optimal Motion Planning for Multiple Robots having Independent Goals. *IEEE Transactions on Robotics and Automation,* Vol. 14, Issue 6, pp. 912-925, ISSN 0882-4967.

Labakhua, L. ; Nunes, U. ; Rodrigues, R. & Leite, F.S. (2006). Smooth Trajectory Planning for Fully Automated Passengers Vehicles, *Proceedings of the 3th International Conference on Informatics in Control, Automation and Robotics (ICINCO),* pp. 89-96, ISBN 972-8865-60-0, Setubal (Portogal), INSTICC press.

Lumelsky, V.J. & Harinarayan, K.R. (1997). Decentralized Motion Planning for Multiple Mobile Robots: the Cocktail Party Model. *Autonomous Robots*, Vol. 4, Issue 1, pp. 121-135, ISSN 0929-5593.

McDonald, M. & Voge, T. (2003). Analysis of Potentials and Limitations of Cybernetic Transport Systems. *Report of TRG Institute*, University of Southampton (UK).

Melluso, M. (2007). Intelligent Fuzzy Lyapunov/EKF Control for Automatic Motion of Ground Vehicles with Non-Holonomic Constraints and Uncertainties. *PhD Thesis*, Dipartimento di Ingegneria dell'Automazione e dei Sistemi, University of Palermo (Italy).

Panfeng, H.; Kai, C.; Janping, Y. & Yangsheng, X. (2007). Motion Trajectory Planning of Space Manipulator for Joint Jerk Minimization, *Proceedings of IEEE International Conference on Mechatronics and Automation,* pp. 3543-3548, ISBN 1-4244-0828-8, Harbin (China).

Raimondi, F.M. & Melluso, M. (2005). A New Fuzzy Dynamic Controller for Autonomous Vehicles with Nonholonomic Constraints. *Robotics and Autonomous Systems,* Elsevier, Vol. 52, pp. 115-131, ISSN 0921-8890.

Raimondi, F.M. & Melluso, M. (2006-a). Fuzzy EKF Control for Wheeled Nonholonomic Vehicles, *Proceedings of 32th IEEE Conference on IECON 2006,* pp. 43-48, ISBN 1-4244-0136-4 , Paris (France).

Raimondi, F.M. & Melluso, M. (2006-b). Robust Trajectory Tracking Control and Localization based on Extended Kalman Filter for Nonholonomic Robots, In: *Advanced Technologies, Research-Development-Application*, edited by Bojan Lalic, pp. 699-724, Pro Literatur Verlag, ISBN 3-86611-197-5, Mammendorf (Germany).

Raimondi, F.M. & Melluso M. (2007-a). Fuzzy Adaptive EKF Motion Control for Non-Holonomic and Underactuated Cars with Parametric and Non-Parametric Uncertainties. *IET Control Theory and Applications,* Vol.1, Issue 5, pp. 1311-1321, ISSN 1751-8644.

Raimondi, F.M. & Melluso M. (2007-b). Fuzzy Cooperative Control of Automated Ground Passenger Vehicles, *Proceedings of IEEE Conference on ETFA 2007,* pp. 1364-1371, ISBN 1-4244-0826-1, Patras (Greece).

Slotine, J.J. & Li, W. (1991). *Applied Nonlinear Control,* Prentice Hall International Edition, ISBN 0-13-040890-5, London UK.

Suzuki, H. (1998). Research Trends of Riding Comfort Evaluation in Japan. *Proceedings of the Institution of Mechanical Engineers part F- Journal of Rail and Rapid Transit,* Vol. 212, Issue 1, pp. 61-72, ISSN 0954-4097.

Motion Control

Edited by Federico Casolo

ISBN 978-953-7619-55-8
Hard cover, 590 pages
Publisher InTech
Published online 01, January, 2010
Published in print edition January, 2010

The book reveals many different aspects of motion control and a wide multiplicity of approaches to the problem as well. Despite the number of examples, however, this volume is not meant to be exhaustive: it intends to offer some original insights for all researchers who will hopefully make their experience available for a forthcoming publication on the subject.

How to reference

In order to correctly reference this scholarly work, feel free to copy and paste the following:

Francesco Maria Raimondi and Maurizio Melluso (2010). Fuzzy Control Strategy for Cooperative Non-holonomic Motion of Cybercars with Passengers Vibration Analysis, Motion Control, Federico Casolo (Ed.), ISBN: 978-953-7619-55-8, InTech, Available from: http://www.intechopen.com/books/motion-control/fuzzy-control-strategy-for-cooperative-non-holonomic-motion-of-cybercars-with-passengers-vibration-a

INTECH
open science | open minds

InTech Europe
University Campus STeP Ri
Slavka Krautzeka 83/A
51000 Rijeka, Croatia
Phone: +385 (51) 770 447
Fax: +385 (51) 686 166
www.intechopen.com

InTech China
Unit 405, Office Block, Hotel Equatorial Shanghai
No.65, Yan An Road (West), Shanghai, 200040, China
中国上海市延安西路65号上海国际贵都大饭店办公楼405单元
Phone: +86-21-62489820
Fax: +86-21-62489821

IntechOpen